

<https://helda.helsinki.fi>

---

## The Unique Blazar OJ 287 and Its Massive Binary Black Hole Central Engine

Dey, Lankeswar

Multidisciplinary Digital Publishing Institute

2019-05-08

---

Dey, L.; Gopakumar, A.; Valtonen, M.; Zola, S.; Susobhanan, A.; Hudec, R.; Pihajoki, P.; Pursimo, T.; Berdyugin, A.; Piirola, V.; Ciprini, S.; Nilsson, K.; Jermak, H.; Kidger, M.; Komossa, S. The Unique Blazar OJ 287 and Its Massive Binary Black Hole Central Engine. Universe 2019, 5, 108.

---

<http://hdl.handle.net/10138/301783>

---

*Downloaded from Helda, University of Helsinki institutional repository.*



*This is an electronic reprint of the original article.*

*This reprint may differ from the original in pagination and typographic detail.*

*Please cite the original version.*

Review

# The Unique Blazar OJ 287 and Its Massive Binary Black Hole Central Engine

Lankeswar Dey <sup>1,\*</sup>, Achamveedu Gopakumar <sup>1</sup>, Mauri Valtonen <sup>2,3</sup>, Stanislaw Zola <sup>4,5</sup>,  
Abhimanyu Susobhanan <sup>1</sup>, Rene Hudec <sup>6,7</sup>, Pauli Pihajoki <sup>8</sup>, Tapio Pursimo <sup>9</sup>,  
Andrei Berdyugin <sup>3</sup>, Vilppu Piirola <sup>2</sup>, Stefano Ciprini <sup>10,11</sup>, Kari Nilsson <sup>2</sup>, Helen Jermak <sup>12</sup>,  
Mark Kidger <sup>13</sup> and Stefanie Komossa <sup>14</sup>

<sup>1</sup> Department of Astronomy and Astrophysics, Tata Institute of Fundamental Research, Mumbai 400005, India; gopu@tifr.res.in (A.G.); s.abhimanyu@tifr.res.in (A.S.)

<sup>2</sup> Finnish Centre for Astronomy with ESO, University of Turku, FI-20014 Turku, Finland; mvaltonen2001@yahoo.com (M.V.); piirola@utu.fi (V.P.); kani@utu.fi (K.N.)

<sup>3</sup> Department of Physics and Astronomy, University of Turku, FI-20014 Turku, Finland; andber@utu.fi

<sup>4</sup> Astronomical Observatory, Jagiellonian University, ul. Orla 171, PL-30-244 Cracow, Poland; szola@oa.uj.edu.pl

<sup>5</sup> Mt. Suhora Astronomical Observatory, Pedagogical University, ul. Podchorazych 2, PL30-084 Cracow, Poland

<sup>6</sup> Czech Technical University in Prague, Faculty of Electrical Engineering, Technicka 2, Prague 166 27, Czech Republic; rene.hudec@gmail.com

<sup>7</sup> Engelhardt Astronomical observatory, Kazan Federal University, Kremlyovskaya street 18, 420008 Kazan, Russia

<sup>8</sup> Department of Physics, University of Helsinki, Gustaf Hållströmin katu 2a, FI-00560 Helsinki, Finland; pauli.pihajoki@helsinki.fi

<sup>9</sup> Nordic Optical Telescope, Apartado 474, E-38700 Santa Cruz de La Palma, Spain; tpursimo@not.iac.es

<sup>10</sup> Space Science Data Center - Agenzia Spaziale Italiana, via del Politecnico, snc, I-00133 Roma, Italy; stefano.ciprini.asdc@gmail.com

<sup>11</sup> Istituto Nazionale di Fisica Nucleare, Sezione di Roma Tor Vergata, I-00133 Roma, Italy

<sup>12</sup> Astrophysics Research Institute, Liverpool John Moores University, IC2, Liverpool Science Park, Brownlow Hill L3 5RF, UK; h.e.jermak@ljmu.ac.uk

<sup>13</sup> Herschel Science Centre, ESAC, European Space Agency, 28691 Villanueva de la Cañada, 28691 Madrid, Spain; mkidger@sciops.esa.int

<sup>14</sup> Max Planck Institut fuer Radioastronomie, Auf dem Huegel 69, 53121 Bonn, Germany; astrokomossa@gmx.de

\* Correspondence: lankeswar.dey@tifr.res.in; Tel.: +91-22-2278-2428

Received: 26 March 2019; Accepted: 6 May 2019; Published: 8 May 2019



**Abstract:** The bright blazar OJ 287 is the best-known candidate for hosting a nanohertz gravitational wave (GW) emitting supermassive binary black hole (SMBBH) in the present observable universe. The binary black hole (BBH) central engine model, proposed by Lehto and Valtonen in 1996, was influenced by the two distinct periodicities inferred from the optical light curve of OJ 287. The current improved model employs an accurate general relativistic description to track the trajectory of the secondary black hole (BH) which is crucial to predict the inherent impact flares of OJ 287. The successful observations of three predicted impact flares open up the possibility of using this BBH system to test general relativity in a hitherto unexplored strong field regime. Additionally, we briefly describe an ongoing effort to interpret observations of OJ 287 in a Bayesian framework.

**Keywords:** general relativity; blazar: OJ 287; black holes

## 1. Introduction

It is now well established that nearly all massive active and normal galaxies contain supermassive black holes (SMBHs) at their centers [1–3]. The SMBH of a typical active galaxy is surrounded by an accretion disk and accretion onto the massive BH fuels the system. The accretion-induced luminosity, arising from its small central region, can be comparable to, and often exceeds, the luminosity of the rest of the galaxy. These central regions are usually referred to as active galactic nuclei (AGNs) [4]. Some AGNs also launch relativistic jets, beams of relativistic ionized matter, along the axis of rotation. If the direction of the jet of an AGN is along our line of sight, we call the AGN a blazar. The radiation we see from a blazar is dominated by the emission from the jet.

As the mergers of galaxies appear to be frequent, it is expected that at the center of some of the galaxies, instead of one SMBH there can be two of them. A number of astrophysical considerations point to the possibility that mergers of two galaxies can lead to the formation of gravitationally bound SMBH binaries [5,6]. While a number of observations have been considered as signatures of SMBH pairs at wide and small separation [7], the blazar OJ 287 (at redshift  $z = 0.304$ ) is the best candidate for hosting a binary SMBH at its center [8,9]. We list below various observational and theoretical pieces of evidence that strongly point to the presence of an SMBH binary in the central engine of OJ 287.

During the 1980s, the Tuorla Observatory started a quasar monitoring program and OJ 287 grabbed attention due to its quasi-periodic doubly-peaked outburst pattern in its optical light curve (LC) [10,11]. In Figure 1 [9], we show the optical LC of OJ 287 which goes all the way back to the year 1888! This data set exists due to the proximity of OJ 287 to the ecliptic and therefore was unintentionally photographed often in the past, providing us with the LC of OJ 287 extending back to  $\sim 130$  years. A visual inspection of the LC reveals the presence of two periodic variations with approximate timescales of 60 and 12 years, which have been confirmed through a detailed quantitative analysis [12]. In the left panel of Figure 1, we mark the 60 year period by a red sinusoidal curve. Additionally, it is possible to infer the presence of regular pairs of outbursts at  $\sim 12$  years interval, where the two peaks are separated by a few years in the LC (see the right panel of Figure 1). The presence of such a double periodicity in the optical LC provided possible evidence for the occurrence of a quasi-Keplerian orbital motion in the blazar. In this description, the 12-year periodicity corresponds to the orbital period timescale and the longer 60-year timescale is associated with the advance of periastron.

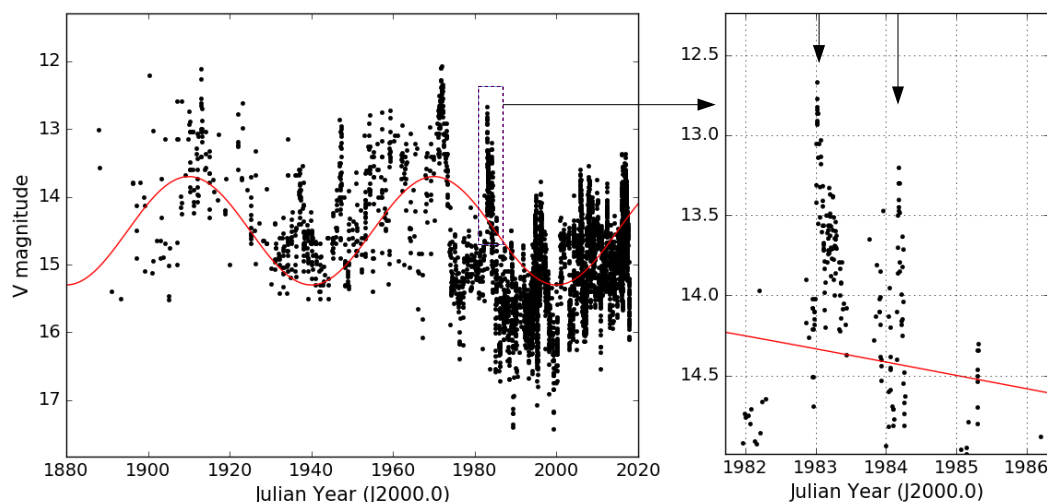


**Figure 1.** The left panel shows the optical LC of OJ 287 from 1888 to 2018. The red sinusoidal curve helps to visualize the longer 60 year periodicity in the LC. The right panel focuses on the LC from 1982 to 1986 for demonstrating the doubly peaked nature of these outbursts [9].

Therefore, a possible model to explain the observed periodicities in the LC naturally involves a secondary black hole that orbits a more massive primary BH in an eccentric orbit [8,13]. Additionally,

the secondary BH impacts the accretion disk of the primary BH twice during one orbit having a (redshifted) period of  $\sim 12$  years (Figure 2). These two impacts produce the two flares that are observed more than a year apart, and such impact flares are repeated during every orbital cycle. We invoke a simple prescription to model the astrophysical process that generates these impact flares. The impact of the secondary BH with the accretion disk releases hot bubbles of gas from the disk on both sides [14,15]. These hot bubbles then expand and cool down until they become optically thin, and the radiation from the entire volume is seen. The radiation is thermal bremsstrahlung at a temperature of  $\sim 10^5$  K [16].

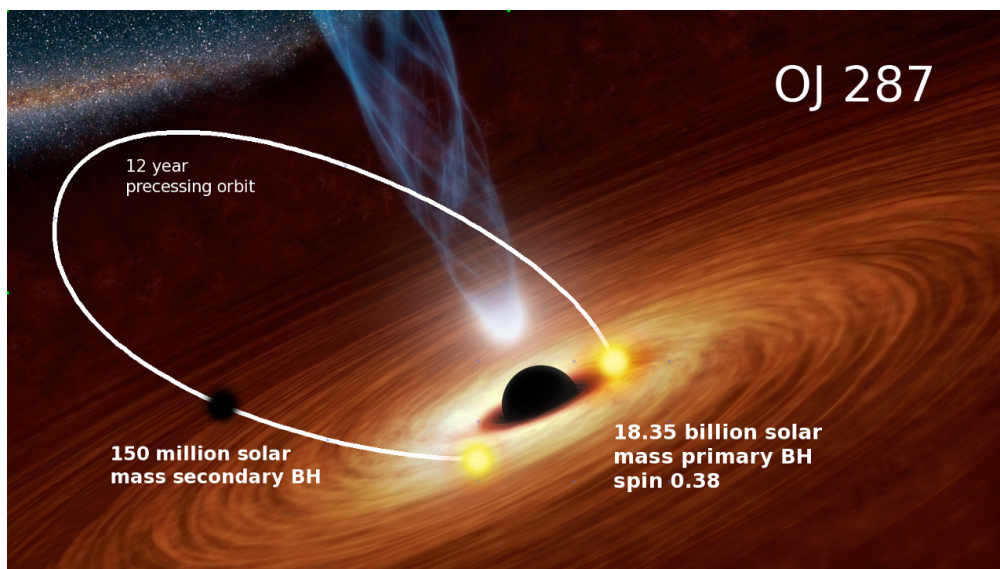


Figure 2. Artistic illustration of the binary black hole system in OJ 287 [9]. ©AAS 2018.

A number of alternative models, available in Refs. Katz [17], Tanaka [18], Britzen et al. [19], did try to explain the observed variations in the LC of OJ 287 that include e.g.; Doppler boosting variation from a turning jet, varying accretion rate, etc. However, the following additional observed features are not explained by other models:

- The flares rise rapidly with the rise time of only about a few days. In contrast, the timescales associated with processes like jet turning are several months to years.
- At the times of impact flares, the degree of polarization always goes down [20,21]. In the BBH model, this is due to an additional unpolarized component associated with the bremsstrahlung radiation at the time of outburst, which is in addition to the long-lived jet emission.
- A natural (and powerful) feature of the BBH impact model is its accurate predictive power. Indeed, the model accurately predicted the starting times for the widely observed 1995, 2005, 2007 and 2015 outbursts [8,20–22]. It is rather difficult to make testable predictions using the alternative models for OJ 287 as they assume that the flares are strictly periodic which puts the prediction off by up to several years. Random deviations around the strictly periodic times do not suit either, as the deviations are predictable.

More details about the alternative models can be found in the Appendix A.

Many aspects of the BBH impact model, detailed in Lehto & Valtonen [8], Sundelius et al. [13], were improved in the subsequent years. These developments include better descriptions for the astrophysical processes causing impact outbursts [23,24], accurate general relativistic orbital description [9] as well as the addition of a large number of archived impact outburst data sets [25]. At present, the BBH dynamics is described using the post-Newtonian approximation to general relativity that incorporates the effects of periastron advance, black hole spin, and GW emission. This detailed prescription makes it possible to test general relativity in strong field regimes not tackled by relativistic binaries present in PSR J0737-3039, LIGO/VIRGO GW events, and stars orbiting

the central massive BH of our galaxy [26–29]. Additional investigations are also being pursued to substantiate the presence of a 1.8 billion solar mass BH in OJ 287. This includes an effort to verify from observations whether the host galaxy of OJ 287 follows the established BH mass-bulge luminosity correlation [30] and employing BH binary scenario to model temporal variations of the jet position angle using high-frequency radio data sets [31–33].

In Section 2, we summarize various developments implemented into the original BBH model and the current state of the model. Section 3 describes various tests of general relativity being pursued or possible with the BBH central engine model for OJ 287. A new, accurate and efficient approach to track the orbit of the secondary BH and to extract astrophysical information from observations are discussed in Section 4. A brief summary and possible future directions are listed in Section 5.

## 2. Construction of the BBH Central Engine Model for OJ 287

This section provides a brief step-by-step description of the BBH central engine model. We begin by showing how fairly basic astrophysical considerations can be invoked to constrain the important parameters of our model. However, we need to invoke the observed outburst timings for accurately estimating various parameters of the BBH impact scenario for OJ 287. How to employ outburst timings and a general relativistic description of the BBH for the above purpose is listed in Sections 2.2 and 2.3. This is followed by the current description of our impact flare model for OJ 287.

### 2.1. Elements of the BBH Model from Astrophysical Considerations

The basic scenario involves a secondary BH that orbits a more massive primary BH and the outbursts occur when the secondary BH impacts the accretion disk of the primary. Interestingly, this scenario allows us to estimate the values of many important model parameters by invoking a few astrophysical considerations. The major flare epochs provide a time sequence of events. It was realized early on that this sequence can be generated by a simple, purely mathematical rule (Lehto & Valtonen [8] or model 1). This rule requires us to consider a particle moving in a Keplerian elliptical orbit, and let the ellipse rotate forward by a constant rate. This leads to a sequence of times when the particle crosses a fixed line in the orbital plane, drawn through the Keplerian focal point of the ellipse. For every value of eccentricity and rotation rate of the ellipse, a time sequence is created and in general, such time sequences need not have anything to do with OJ 287 observations. However, if we choose eccentricity and precession rate to be  $\sim 0.7$  and  $\sim 39$  degrees per orbit, respectively, we get a sequence of epochs that matches fairly well with the OJ 287 flare timings. The physical and astrophysical implications of the above conclusion were explored in Lehto & Valtonen [8] (model 2). Clearly, the crossing of the line can be naturally associated with the crossing of an inclined plane in a binary system. Further, what actually generates the signal is not of great importance as far as the determination of the orbit is concerned [34]. Importantly, if we invoke General Relativity (GR) to explain the forward precession rate, we get a very robust value for the total mass of the underlying system in OJ 287.

Let us now add one more assumption. Assume that the two periodicities (12 and 60 years) in the light curve are related to the two periodicities in the system, the orbital period and the precession period. It does not matter what the mechanism is. Naturally, the inferred 60-year periodicity of the LC may be associated with half of the orbital precession period as the precession effects are expected to be symmetric about the accretion disk plane (the orbital precession arises from the post-Keplerian orbital trajectory for the secondary BH). It is straightforward to estimate the orbital precession rate per orbit in degrees to be  $\Delta\phi \sim 12 \times 180/60 \text{ deg} = 36 \text{ deg}$  where we let the orbital period of the binary to be  $\sim 12$  years. Invoking GR to explain the above  $\Delta\phi$  value can lead to an estimate for the total mass of the BBH, provided we have an estimate for the orbital eccentricity. It is reasonable to use the minimum temporal separation between the two peaks of the doubly-peaked outbursts to constrain the eccentricity. This is the value we get from the purely mathematical model. The ratio of the minimum time interval between the two nearby impact flare peaks and the orbital period should be larger for



orbits with small eccentricities. In contrast, this ratio is expected to be smaller for eccentricity values close to unity. It turns out that the optimal value for orbital eccentricity is  $\sim 0.7$  from observations. We may now provide an estimate for the total mass ( $M$ ) of the BBH system in OJ 287 with the help of the following expressions for the orbital period ( $P$ ) and the precession rate ( $\Delta\phi$ ), namely

$$P^2 = \frac{4\pi^2 a^3}{G M}, \quad (1)$$

$$\Delta\phi = \frac{6\pi G M}{c^2 a (1 - e^2)}, \quad (2)$$

where  $a$  is the semi-major axis of the orbit. With the help of the inferred  $P$ ,  $\Delta\phi$  and  $e$  estimates, we get the approximate total mass of the system  $M \sim 2 \times 10^{10} M_\odot$  after eliminating the parameter  $a$  from the above two equations. Recall that Equation (2) provides only the leading order GR contributions to periastron advance, characterized by  $\Delta\phi$ . The higher order corrections provide additional positive contributions to  $\Delta\phi$  and therefore the above  $M$  estimate is a slight overestimation. Let us emphasize that no additional astrophysical considerations are invoked to obtain the above  $M$  estimate. Additionally, it is possible to provide an estimate for the mass of the secondary BH by employing the astrophysics of the impact and the strength of the outburst signal [14,16]. The use of the observed outburst luminosity of 5.6 mJy for the 2007 outburst and the Lehto & Valtonen [8] model lead to an estimate for the secondary BH mass to be  $m_{\text{sec}} \sim 1.4 \times 10^8 M_\odot$  [16]. Let us emphasize that these estimates were extracted without really employing the accurate timing data from the observed outbursts from OJ 287, only the first order fit to the Keplerian orbital dynamics with the GR forward precession. More precise estimates of the BBH parameters by explicitly using outburst timings are given in Section 2.4.

## 2.2. Details of BBH Central Engine from the Timing of Impact Outbursts

We now move on to describe how we estimate various parameters of the BBH central engine model using the outburst timings. This requires us to bring in additional astrophysical considerations as the outbursts do not take place just at the epochs of secondary BH impacts. Such impacts are expected to result in the creation of two hot plasma bubbles which come out from both sides of the accretion disk. These plasma bubbles expand, cool, and after a time delay, become optically thin. This is when the radiation can escape the gas plasma bubble and manifest as the impact flare. The time interval taken by these bubbles to become optically thin is termed as the ‘time delay’ and it clearly affects the observed starting epoch of an outburst. Therefore, accurate modeling of the time delay is crucial for us.

A calculation to compute the above time delay was first provided in Lehto & Valtonen [8]. Subsequently, Ivanov et al. [14] carried out a hydrodynamic simulation of the impact and the release of a hot cloud of plasma from the disk. Their simulation showed that plasma cloud is released from both sides of the disk, one bubble bursting out to the backward direction relative to the motion of the secondary, the other following the orbit of the secondary. The physical properties of the bubbles were calculated and they matched well with what is expected from simple analytic arguments. Unfortunately, Ivanov et al. [14] did not carry out their calculation far enough to reach the radiation outburst stage. However, they estimated that the resulting flare should correspond to the Eddington luminosity of the secondary BH at the maximum brightness as argued in Lehto & Valtonen [8]. This calculation incorporates the idea that the secondary BH impact creates a compressed spherical blob of plasma. The optical outburst occurs when such a blob expands by a factor of  $\tau^{4/7}$  where  $\tau$  is the initial optical depth and this expansion essentially provides the time delay in terms of the accretion disk and BH parameters [8,35]. Specifically, the time delay depends on the mass of the secondary BH ( $m_{\text{sec}}$ ), the relative velocity of the secondary BH with respect to the accretion disk ( $v_{\text{rel}}$ ) at the time of impact and density ( $n$ ) and thickness ( $h$ ) of the disk. The expression for the time delay given in Lehto & Valtonen [8] reads

$$t_{\text{del}} = d m_{\text{sec}}^{26/21} v_{\text{rel}}^{-355/84} h^{13/21} n^{102/112}, \quad (3)$$

where  $d$  is a parameter called ‘delay parameter’ which depends on the accretion disk properties. Note that the time delay is a function of the secondary mass. The time delay and therefore the secondary mass is also determined as a part of the orbit solution. This method is in no way related to the secondary mass determination using the brightness of the flare. It is remarkable that the two methods give essentially the same value within the 10 percent uncertainty. The secondary mass value also agrees with the limit provided by the long term stability requirement. It was argued that the disk becomes unstable if the primary versus secondary mass ratio is less than 100 [16]. It is customary to adapt the  $\alpha_g$  disk, in which the viscosity is proportional to the gas pressure [36]. In this model, the properties of the accretion disk are uniquely defined by the central mass, the accretion rate of the primary ( $\dot{m}$ ) and the viscosity parameter ( $\alpha$ ). Using the disk model, Lehto & Valtonen [8] calculated the variations in the disk properties like  $h$  and  $n$  with the distance from the central BH. This allows one to obtain reasonable estimates for  $h$  and  $n$  of the accretion disk at the impact site, provided the impact site distance ( $R_{\text{imp}}$ ) from the central BH is available. A general relativistic description for the BBH orbit should be able to provide  $R_{\text{imp}}$  and  $v_{\text{rel}}$  at the time of impact and therefore, BBH dynamics essentially provides an estimate for the time delay. We need to invoke GR, as the BBH of the model experiences a periastron advance of  $\sim 39^\circ$  per orbit. In comparison, the measured advance of periastron for the double pulsar is  $\sim 0.005^\circ$  per orbit [37]. In summary, our Equation 3 provides an astrophysically relevant estimate for the time delays for different impact epochs, essentially from a general relativistic BH binary description.

An additional astrophysical aspect needs to be incorporated while dealing with the ‘time delays’. The tidal force of the approaching secondary BH causes the accretion disk to be pulled up towards the secondary. This forces the impacts to occur at earlier epochs compared to a scenario where we neglect the tidal deformation of the disk and this time difference is termed as ‘time advance’ ( $t_{\text{adv}}$ ) (see Valtonen [23] for details). In practice, we let the accretion disk to lie in a fixed plane as the  $y = 0$  plane in Figure 3 [9]. In our approach, the observed starting time of the impact flare is given by

$$t_{\text{out}} = t_{\text{imp}} - t_{\text{adv}} + t_{\text{del}}. \quad (4)$$

where  $t_{\text{imp}}$  stands for the time of the disk impact, obtainable from BBH orbital dynamics. How we describe the BBH dynamics is explained in the next subsection.

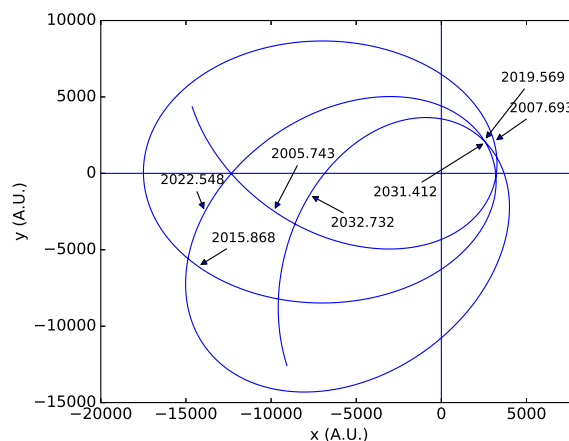


**Figure 3.** The typical orbit of the secondary BH in OJ 287 in 2005–2033 window. The primary BH (Schwarzschild radius  $R_S \sim 362$  AU) is situated at the origin with its accretion disk in the  $y = 0$  plane. The average distance of periastron is  $\sim 9 R_S$  and the binary is going to merge within 10,000 years. The locations of the secondary BH at the time of different outburst epochs are marked by arrow symbols. The time-delay effect is clearly visible, while close inspection reveals that these delays for different impacts are different [9]. ©AAS 2018

### 2.3. General Relativistic Orbital Trajectory for the Secondary BH

We employ the post-Newtonian (PN) approximation to GR to describe the evolution of secondary BH trajectory in the strong gravitational field of the primary BH. The PN approximation provides dynamics of BH binaries as corrections to the Newtonian dynamics in powers of  $(v/c)^2 \sim GM/(c^2 r)$ , where  $v$ ,  $M$ , and  $r$  are the characteristic orbital velocity, the total mass, and the typical orbital separation of the binary, respectively. In a convenient center of mass frame, the post-Newtonian equations can be written in the form [38,39]

$$\ddot{\mathbf{x}} \equiv \frac{d^2 \mathbf{x}}{dt^2} = \ddot{\mathbf{x}}_0 + \ddot{\mathbf{x}}_{1\text{PN}} + \ddot{\mathbf{x}}_{2\text{PN}} + \ddot{\mathbf{x}}_{3\text{PN}} + \ddot{\mathbf{x}}_{2.5\text{PN}} + \ddot{\mathbf{x}}_{3.5\text{PN}} + \ddot{\mathbf{x}}_{4\text{PN}(\text{tail})} + \ddot{\mathbf{x}}_{4.5\text{PN}} + \ddot{\mathbf{x}}_{\text{SO}} + \ddot{\mathbf{x}}_{\text{Q}} + \ddot{\mathbf{x}}_{4\text{PN}(\text{SO-RR})}, \quad (5)$$

where  $\mathbf{x} = \mathbf{x}_1 - \mathbf{x}_2$  gives the relative separation vector between the two BHs with masses  $m_1$  and  $m_2$  in the center-of-mass frame. The familiar Newtonian contribution, denoted by  $\ddot{\mathbf{x}}_0$ , is given by  $\ddot{\mathbf{x}}_0 = -\frac{Gm}{r^3} \mathbf{x}$ , where  $m = m_1 + m_2$ ,  $r = |\mathbf{x}|$ . Note that nPN contributions provide  $\mathcal{O}((v/c)^{2n})$  correction terms.

The 1PN, 2PN and 3PN terms that appear in the first line of Equation (5) are conservative in nature and essentially force the periastron of the orbit to precess. The contributions appearing in the second line of Equation (5), namely, 2.5PN, 3.5PN, 4PN(tail), and 4.5PN terms, are due to the emission of GWs from the binary system. These contributions force the orbital period and eccentricity to decay with time. Dey et al. [9] showed that the contributions of PN terms higher than 4.5 are negligible for the binary dynamics in OJ 287. The effects of BH spin enter the above equation in the third line and the  $\ddot{\mathbf{x}}_{\text{SO}}$  term provides the general relativistic spin-orbit interactions at 1.5PN and 2.5PN orders. These terms make the orbital plane of the secondary and spin of the primary to precess while the  $\ddot{\mathbf{x}}_{4\text{PN}(\text{SO-RR})}$  term stands for the spin-orbit radiation reaction terms. The classical spin-orbit term or the quadrupolar term is denoted by  $\ddot{\mathbf{x}}_{\text{Q}}$  and how we plan to test the celebrated *Black Hole no-hair theorem* with its help will be discussed in Section 3.2. We note that the  $\ddot{\mathbf{x}}_{4\text{PN}(\text{tail})}$  contributions are somewhat different from the other reactive terms. This term arises due to the scattering of quadrupolar GWs from the space-time curvature created by total mass (monopole) of the system and hence depends, in principle, on the entire history of the system; they are called hereditary contributions [40]. A closed form expression for these contributions does not exist and an effective way of incorporating such contributions is discussed in Dey et al. [9].

We move on to describe how we estimate various parameters of the BBH central engine model for OJ 287 [23]. The orbital trajectory of the secondary BH is determined by numerically integrating Equation (5). Initially, we determine the orbit using certain ‘guesstimates’ for various parameters as described in Section 2.1. From such an orbital description, the times of impacts of the secondary BH with the accretion disk are calculated (these are the times when the orbit crosses the accretion disk plane  $y = 0$  as in Figure 3). This allows us to obtain the starting times of various outbursts, calculated using Equation (4). Thereafter, we carefully check if these calculated starting times agree with the well-observed outburst epochs within uncertainties. If not, the parameters are changed and the whole procedure is repeated. When all the outburst timings, determined by tracking the orbital trajectory of the secondary BH, match with the observed ones, the parameters are taken to be a solution. In Figure 3 we display a typical orbit of the binary system in OJ 287.

### 2.4. The Most up to Date Description of the BBH Central Engine

Currently, we have accurate measurements for the starting times of 10 well-observed outbursts at our disposal to constrain the binary orbit. These 10 outburst starting times are given in Table 1 with the observational uncertainties [9].



**Table 1.** Extracted starting times of the well-observed optical outbursts of OJ 287 [9]. ©AAS 2018.

Outburst Times with Estimated Uncertainty (Julian Year)
1912.980 $\pm$ 0.020
1947.283 $\pm$ 0.002
1957.095 $\pm$ 0.025
1972.935 $\pm$ 0.012
1982.964 $\pm$ 0.0005
1984.125 $\pm$ 0.01
1995.841 $\pm$ 0.002
2005.745 $\pm$ 0.015
2007.6915 $\pm$ 0.0015
2015.875 $\pm$ 0.025

Using these 10 outburst times, we determine the binary system parameters using the above-listed procedure. These parameters include the mass of the primary BH  $m_1$ , the mass of the secondary BH  $m_2$ , the Kerr parameter of the primary BH  $\chi_1$ , present orbital eccentricity  $e_0$ , the rate of advance of pericenter per orbit  $\Delta\phi$  and the orientation of the semi-major axis  $\Theta_0$  in 1856 (starting time of orbit integration). Additionally, we can estimate two more parameters related to the effects of astrophysical processes that are associated with the accretion disk impact of the secondary BH. These two parameters are  $d$  and  $h$  where  $d$  is the delay parameter present in Equation (3), while the disk thickness parameter  $h$  is a scale factor with respect to the “standard” model of Lehto & Valtonen (1996). The solutions for these parameters are listed below in Table 2 [9].

**Table 2.** Parameters of the orbit solution [9]. ©AAS 2018.

Parameter	Value	Unit
$m_1$	18348	$10^6 M_\odot$
$m_2$	150.13	$10^6 M_\odot$
$\chi_1$	0.381	
$e_0$	0.657	
$\Delta\Phi$	38.62	deg
$\Theta_0$	55.42	deg
$h$	0.900	
$d$	0.776	

It is possible to derive two additional quantities using the extracted parameters listed in Table 2. They are the present orbital period of the binary orbit  $P_{\text{orb}} = 12.06$  years and the rate of orbital period decay  $\dot{P}_{\text{orb}} = 0.00099$ . These estimates suggest that the binary BHs will merge within 10,000 years. Additionally, these accurate estimates allow us to predict the start of the next impact flare outburst to be on 29 July 2019.

### 3. Tests of GR Using OJ 287

Testing Einstein’s general theory of relativity in the vicinity of strong gravitational fields is an important endeavor [41]. This is mainly to explore any possible deviations from Einstein’s predictions for the behavior of gravitational fields in dynamical and strong gravity scenarios. Compact binaries like PSR B1913+16 pioneered the efforts to test GR in strong field regimes [26]. Recent observations of GWs from merging BH-BH and Neutron Star–Neutron Star binaries are allowing the test of GR in ultra-strong and dynamical gravitational fields [42]. It turns out that OJ 287 observations can be used to test GR in the yet-to-be-explored strong field regime as displayed in the left panel of Figure 4.

### 3.1. First Indirect Evidence for GW Emission from BH-BH Binaries

In Einstein's GR, orbiting compact objects should emit GWs. This causes the binary to lose its orbital energy and angular momentum which forces the decay of its orbital period and eccentricity. The existence of GWs from inspiralling NS-NS binaries was demonstrated by the long-term radio timing of PSR B1913+16 [43]. The first indirect evidence for the emission of GWs from orbiting BH-BH binary was provided by the 2007 monitoring of the predicted OJ 287 impact flare [20]. In the BBH central engine model, the secular changes in the secondary BH trajectory can change the computed times of its impact with the accretion disk of the primary BH. This can naturally shift the expected starting epochs of the impact flare outbursts.

The indirect evidence for the presence of GW emission in OJ 287 was demonstrated with the help of PN-accurate orbital dynamics, given symbolically by Equation (5). We note that the starting time of this outburst was predicted to be 13 September 2007, with an uncertainty of two days, while employing the fully 2.5PN accurate equations of motion. However, the BBH model predicted the start of the 2007 outburst some 20 days later (in early October 2007) when the orbit of the secondary BH was computed without incorporating the 2.5PN order radiation reaction terms in the orbital dynamics. The 2007 observational campaign for OJ 287, starting on 4 September, did witness the beginning of the expected outburst on 12 September 2007. This crucial observation provided the indirect evidence for the presence of GW emission from the BH-BH system in OJ 287 [20].

### 3.2. Testing the BH 'No-hair' Theorem during the Present Decade

The celebrated Black Hole 'no-hair' theorem states that a rotating BH can be completely described by its mass and angular momentum [44]. This implies that we do not require any equation of state to describe the properties of BHs as we need to do for neutron stars. In other words, the multipole moments of a rotating BH can be determined in terms of their mass and angular momentum alone (BHs have 'no hair') and prompted the formulation of the following test of the theorem [45]. The test involves estimating the mass, the spin and the quadrupole moment of a rotating astrophysical BH from observations. It turns out that the dimensionless quadrupole moment ( $q_2$ ) of a BH in GR is related to its Kerr parameter ( $\chi$ ) by a very unique relation, namely  $q_2 = -\chi^2$ . There are on-going efforts to test this relation with the help of GW observations [46], X-ray binary [47], black hole images [48] and by timing BH-pulsar systems in the SKA era and observing stars orbiting galactic center BH during the TMT era.

We propose to test the above relation by replacing the primary BH quadrupole moment that appears in the  $\ddot{x}_Q$  term by

$$q_2 = -q\chi^2, \quad (6)$$

where the minus sign reflects the oblate nature of a rotating BH and in GR  $q \equiv 1$  [49]. The plan is to extract the value of the free parameter  $q$  from the observed impact flare timings and at present, we can constrain the value of  $q$  to be  $1 \pm 0.5$ . Interestingly, an accurate determination of the starting time of the next impact flare should allow us to constrain the  $q$  value at the 10% level. This is possible because the starting time of the expected 2019 outburst is highly correlated with the  $q$  value [9]. In the right panel of Figure 4, we show the correlation between the parameter  $q$  and the starting time of 2019 outburst and the outburst will start on 29 July 2019, if the theorem holds.

Unfortunately, OJ 287 will be very close to the Sun at the predicted time and it is impossible to observe it from any ground-based observatory. The best strategy is to observe OJ 287 by employing space-based telescopes which are located far from the Earth during late July/early August 2019. Indeed, we have an approved warm Spitzer Space Telescope proposal for observing OJ 287 during the epoch when the impact flare magnitude is expected to peak. We have argued that the expected 2019 outburst light curve should be similar to that of 2007 [9]. This opens up the possibility of determining the epoch of the rising part of this outburst even if we miss its actual observation. In the next section, we outline a new method to describe the dynamics of the BBH in OJ 287.

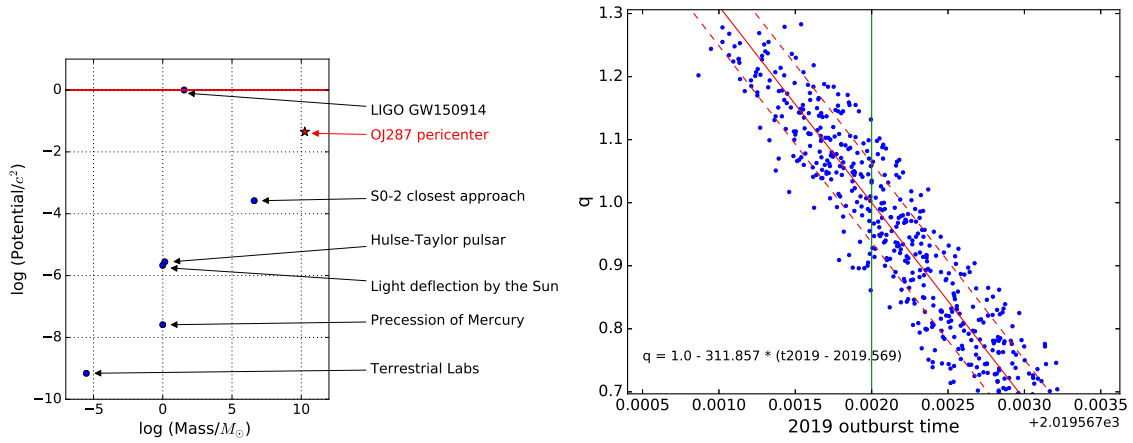


**Figure 4.** The left panel plots the dimensionless gravitational potential against the gravitating mass in solar mass units for systems used to test Einstein’s GR; The unique position of OJ 287 is clearly visible. The right panel shows the correlation between the value of the  $q$  parameter and the starting time of 2019 outburst where each point represents a possible solution of the binary in OJ 287. The solid red line shows our fit to the observed correlation and the dashed red lines indicate its  $1\sigma$  deviation (the fit equation is given in the lower-left corner of the plot). The green vertical line represents the expected outburst starting time from the model [9]. ©AAS 2018.

#### 4. Describing OJ 287’s BBH Dynamics via GW Phasing Prescription for Eccentric Binaries

The prospects of pursuing strong field tests of GR prompted us to develop an improved prescription to track the secondary BH trajectory in an accurate and computationally inexpensive manner. This is a crucial requirement as we plan to employ Bayesian methods to test GR using OJ 287 observations. Recall that the Bayesian approach demands computation of the likelihood function millions of times that involves a similar number of BH trajectory computations. At present, such large scale computations are not viable as we blindly solve Equation (5) numerically for following the secondary BH which is computationally expensive. We adapt the GW phasing approach, detailed in Refs. [50,51], that provides accurate orbital phase evolution for compact binaries inspiralling along PN-accurate precessing eccentric orbits. The phasing approach focuses on the accurate temporal orbital phase evolution, a crucial requirement for constructing GW templates for such binaries. This feature is crucial for making accurate predictions for the impact flare timings as these flares occur when the secondary crosses the accretion disk of the primary at constant orbital phase angles like  $0, \pi, 2\pi, \dots$ . Therefore, accurate BBH orbital phase determination should lead to precise predictions for the impact flare epochs.

The GW phasing formalism provides an efficient way of solving both the conservative and reactive contributions to the orbital dynamics, specified by the first and second lines in Equation (5). It turns out that the 3PN-accurate conservative part of this orbital dynamics is integrable and admits a Keplerian-type parametric solution as detailed in Refs. [52–54]. The existence of such a 3PN-accurate Keplerian-type parametric solution allows us to express the orbital phase as

$$\phi(t) = \lambda + W(u(l), \mathcal{E}, \mathcal{J}), \quad (7)$$

where  $u$  and  $l$  are the eccentric and mean anomalies of the PN-accurate Keplerian parametrization, while  $\mathcal{E}$  and  $\mathcal{J}$  stand for the conserved orbital energy and the angular momentum, respectively. The split of the angular variable  $\phi$  ensures that the contributions due to periastron advance remain linear in  $l$  while the  $2\pi$ -periodic  $W(u)$  part analytically models orbital time scale variations in  $\phi$ . These considerations allow us to write  $\lambda = (1 + k)l$ , where  $k$  provides the dimensionless rate of periastron advance per orbit. An additional equation is required to specify how  $u$  varies with  $l$  which allows us to

model explicitly the temporal evolution of  $\phi$  as  $l = n(t - t_0)$  where  $n$  is the mean motion. In practise, we solve 3PN-accurate Kepler equation to find  $u(l)$  and this equation can be symbolically written as

$$l = u - e_t \sin u + l_3(u, \mathcal{E}, \mathcal{J}). \quad (8)$$

In this equation,  $l_3$  stands for the 3PN order corrections to the usual Newtonian Kepler equation, namely  $l = u - e_t \sin u$  and  $e_t$  denotes certain ‘time-eccentricity’ parameter of the Keplerian-type parametric solution to PN-accurate orbital dynamics.

Detailed computations reveal that the secular variations to  $\mathcal{E}$  and  $\mathcal{J}$  due to the addition of reactive contributions to the orbital dynamics, namely the second line in Equation (5), are identical to the PN-accurate expressions for far-zone energy and angular momentum fluxes. This is a highly desirable result as the far-zone energy and angular momentum fluxes are available to higher PN orders. This allowed us to model orbital dynamics of compact binaries inspiralling under the influence of GW emission at the 2PN order while moving along 3PN-accurate eccentric orbits, as described by the first and second line contributions in Equation (5). Further, the approach allowed us to tackle the spin effects separately. In practise, we employ the mean motion  $n$  and  $e_t$  to characterize the orbit in place of  $\mathcal{E}$  and  $\mathcal{J}$  and GW phasing approach provides differential equations for  $n$  and  $e_t$ . At present, we include all the relevant 3PN (relative) contributions to the above two differential equations with the help of Refs. [55,56]. Additionally, the approach provides differential equations to describe the secular evolution to  $\lambda$  and  $l$ . Therefore, we solve the resulting four ordinary coupled differential equations along with PN-accurate Kepler equation to obtain  $u$  as a function of time. This allows us to obtain an accurate and efficient way of describing temporal evolution to  $\phi$ , caused by various PN contributions in Equation (5).

It is now straightforward to compute the time when the secondary BH crosses the accretion disk of the primary ( $t_{\text{imp}}$ ). This is obtained by finding out the epochs at which  $\phi$  becomes an integer multiple of  $\pi$  like  $0, \pi, 2\pi, 3\pi, \dots$ . This is justifiable as we let the accretion disk plane be the sky plane and define the ascending node as the point where secondary BH crosses the accretion disk plane. After gathering the impact epoch, we invoke Equation (4) to calculate the actual starting time of the associated outburst which we can compare with observational data given in Table 1. This way we can model the observational data with the BBH central engine model for OJ 287 while adapting the GW phasing approach.

Few comments are in order. Note that when we obtain the secondary BH trajectory by numerically integrating Equation (5), we have to solve three complicated second order differential equations for three components of the position vector ( $\mathbf{x}$ ) which is equivalent to solving six first order equations. However, we solve only four first-order orbital averaged differential equations in the phasing approach. Additionally, we can use larger time step for the integration of these four equations as the temporal evolution for  $n$  and  $e_t$  occurs slowly on a GW radiation reaction time scale of a few thousand years. However, the position vector ( $\mathbf{x}$ ) changes rapidly on an orbital time scale while numerically integrating Equation (5). This forces us to use finer time steps for the integration. These considerations ensure that accurate and efficient computation of secondary BH trajectory when we adapt GW phasing approach to deal with BBH central engine in OJ 287. A manuscript that details the above approach and an associated publicly available code is in preparation.

## 5. Summary

The bright (and unique) blazar OJ 287 is a natural candidate for hosting an SMBBH at its center. Its optical LC shows quasi-periodic doubly peaked high brightness flares with a period of  $\sim 12$  years which leads to the BBH central engine model for OJ 287. This model accurately predicted the starting times of 2007 and 2015 outbursts. At present, we employ a sophisticated PN-accurate orbital description and a detailed impact model to calculate the binary orbit and to predict the epochs of future outbursts. The next flare is predicted to peak around 31 July 2019. The predictive power of our BBH central engine

model can be used to test different aspects of GR. A decade ago, our model provided the first indirect evidence for the emission of GWs from black hole binaries prior to the monumental direct detection of GWs from merging BH binaries by the LIGO-Virgo consortium. Additionally, the BBH central engine model provided the test of the BH no-hair theorem and precise measurement of the starting time of the 2019 outburst will allow us to test no-hair theorem at  $\sim 10\%$  level. We briefly presented an accurate and computationally efficient method to track the secondary BH trajectory. This is being incorporated into a Bayesian framework to fit the observational data with the BBH central engine model. These developments should allow us to pursue unique strong field tests of GR with OJ 287 observations. A description of alternative models of OJ 287 is also given in the Appendix A.

**Author Contributions:** L.D., A.G., M.V, P.P. and A.S. developed various facets of the astrophysical model while others contributed with observational efforts. All authors discussed the results and commented on various aspects of the manuscript.

**Funding:** This research received no external funding.

**Acknowledgments:** L.D. thanks FINCA and acknowledges the hospitality of University of Turku, Finland. S.Z. acknowledges NCN grant No. 2018/29/B/ST9/0793.

**Conflicts of Interest:** The authors declare no conflict of interest.

## Abbreviations

The following abbreviations are used in this manuscript:

GW	Gravitational Wave
SMBBH	Supermassive binary black hole
BBH	Binary black hole
SMBH	Supermassive black hole
AGN	Active galactic nucleus
LC	Light curve
GR	General Relativity

## Appendix A. Alternative Models for OJ 287

In what follows, we briefly discuss various alternative models proposed for OJ 287 over the years, how those models tried to explain the observed variability in OJ 287 and what are their shortcomings. We begin by a scenario where a companion black hole orbits the primary inside the accretion disk of the primary, detailed in Sillanpää et al. [11]. It produces a periodic sequence of outbursts via increased accretion flow into the primary. The typical time scale of the rise of the flare is about one month, in contrast to the observed one-day time scale. This is a viable mechanism for explaining the variations in the background level of OJ 287, as was shown first by Sundelius et al. [13]. Another mechanism suitable for explaining background level variations is a model first proposed by Katz [17]. In this model, the secondary influences the orientation of the accretion disk, which is presumably connected to the jet in a way that causes a jet wobble in tune with the disk variations. This provides a good description for the background level variation in the time scale of decades [32]. However, attempts to connect this mechanism with flares have failed. For example, the similar kind of precessing jet model of Britzen et al. [19] explains the timing of only two of the 10 brightest optical flares in the historical light curve of OJ 287. The other eight bright flares have occurred during the periods when OJ 287 should have been in a quiet state according to this model. Therefore, its rate of success is no better than being accidental. We note that the model predicted six periods of activity lasting about four years each over the last 140 years of observed time span. The random rate of  $24/140 \sim 1/6$  is not very different from  $1/5$ , the success rate of this model. Additionally, the model predicts roughly one year for the flux rise which is very different from the observed one day time scale.

Valtaoja et al. [57] proposed a hybrid model which requires the secondary impacts of the accretion disk to produce a flare only at every other disk crossing. They assume that the disk is sharply truncated



between the two impacts points, and only the closer impact produces the flare. On the other hand, they assume that the more distant crossings should be more efficient in generating tidal responses in the disk than the closer impacts. This is clearly counter-intuitive to what is generally accepted about the tidal responses. In order that the sharp disk truncation would help to create two kinds of flares, the impact flare and the tidal flare, Valtaoja et al. [57] have to assume that the major axis of the binary does not precess which puts an unrealistically low upper limit on the primary BH mass. If there were precession, it would gradually remove both impact points beyond the truncation radius, or bring both impacts points inside the truncation radius, depending on where the truncation happens exactly. Note that even a few degrees of orbital precession should have observational implications; the model demands periastron advance to be a fraction of a degree per orbital revolution. This limits the primary mass to be  $M \sim 2 \times 10^8 M_{\odot}$  and the secondary black hole mass has to be very similar to the above estimate in order to produce the impact flares of the required magnitudes [8]. In other words, the model essentially requires a comparable mass BH binary in OJ 287. Interestingly, The accretion disk in such a system is unstable within a few orbital revolutions [16] which contradicts the fact that OJ 287 has been observed over 100 years.

Interestingly, there exists a constant orbital period BH binary model where the rms prediction error has been around 1.5 years Valtaoja et al. [57]. A good illustration of this feature was its prediction that a major flare should occur in the fall of the year 2006. In fact, the latter part of 2006 was the time of a major dip in the light curve indicating that OJ 287 was exceptionally quiet. The major flare happened a year earlier, at the time predicted by an earlier version of our binary black hole model Sundelius et al. [13]. This model predicted the whole LC of OJ 287 from the year 1900 to the year 2030, and so far it has been spectacularly successful [58]. In contrast, there exists a class of models which ignores the fact that the flare times are predictable even though they have been predicted with the rms accuracy of 16 days since 1988 [59]. The unpredictability of OJ 287 has been advocated by Villforth et al. [60] and more recently by Qian [61]. Besides being predictable, OJ 287 displays two clear periodicities of roughly 12 and 60 years when one performs a regular Fourier analysis of its light curve [12]. Note that Goyal et al. [62] did not detect such periodicities and this is attributable to the use of plate calibration curves (that is, they picked the observations only when OJ 287 was just above the plate limit) instead of the OJ 287 historical light curve. Indeed, this effort showed that the 12 and 60 yr cycles are not due to the changing plate material or choice of exposure times in the historical plate archives. We note that quasi-periodic oscillations with this time structure were eliminated by Valtonen et al. [58] at a high significance level.

In summary, we infer that various alternative models can explain some of the observational aspects of OJ 287 and usually fail to explain many other features. In contrast, the BBH impact model of Lehto & Valtonen [8] explains most of the features present in the optical LC of OJ 287, like sharp rise of flares, decrease in degree of polarisation during flares, the long term periodic variations etc. This model can also explain the features present in high frequency radio observations of the jet of OJ 287 [31–33]. Most importantly, our model has accurately predicted the starting times of the widely observed 1995, 2005, 2007 and 2015 outbursts [8,20–22] which places the model in much stronger ground than any of the alternative models. Let us note that the 1994 flare was also predicted successfully by Sillanpää et al. [11], based on their constant period BBH model. This idea has not worked for the later flares as they are clearly not periodic. In fact, the constant period model predicted a flare during 2018, while OJ 287 actually went to one of its deepest minimum flux values during that year. However, many flares have also been discovered in the historical light curve since the completion of the impact model in early 1995 [63]. They all follow the expected pattern, and in this sense there have been many more successful predictions than what was listed earlier. The most prominent of the recently discovered flares is the 1957–1959–1964 triple, of which only the middle one was known in 1995 when the impact model was first presented. The triple occurs when the major axis of the binary is lined up with the disk plane. It happens about every 60 years. Interestingly, we are at present in the middle of the 2015–2019–2022 triple. Such triples do not exist in other models proposed so far.

## References

1. Kormendy, J.; Richstone, D. Inward Bound—The Search For Supermassive Black Holes In Galactic Nuclei. *Annu. Rev. Astron. Astrophys.* **1995**, *33*, 581. [[CrossRef](#)]
2. Ferrarese, L.; Ford, H. Supermassive Black Holes in Galactic Nuclei: Past, Present and Future Research. *Space Sci. Rev.* **2005**, *116*, 523–624. [[CrossRef](#)]
3. Graham, A.W. Galaxy Bulges and Their Massive Black Holes: A Review. *Galact. Bulges* **2016**, *418*, 263–313.
4. Kembhavi, A.K.; Narlikar, J.V. *Quasars and Active Galactic Nuclei: An Introduction*; Cambridge University Press: Cambridge, UK, 1999; ISBN 0521474779.
5. Begelman, M.C.; Blandford, R.D.; Rees, M.J. Massive black hole binaries in active galactic nuclei. *Nature* **1980**, *287*, 307. [[CrossRef](#)]
6. Merritt, D.; Milosavljević, M. Massive Black Hole Binary Evolution. *Living Rev. Relativ.* **2005**, *8*, 8. [[CrossRef](#)]
7. Komossa, S.; Zensus, J.A. Compact object mergers: Observations of supermassive binary black holes and stellar tidal disruption events. *Star Clust. Black Holes Galaxies across Cosm. Time* **2016**, *312*, 13 [[CrossRef](#)]
8. Lehto, H.J.; Valtonen, M.J. OJ 287 Outburst Structure and a Binary Black Hole Model. *Astrophys. J.* **1996**, *460*, 207. [[CrossRef](#)]
9. Dey, L.; Valtonen, M.J.; Gopakumar, A.; Zola, S.; Hudec, R.; Pihajoki, P.; Ciprini, S.; Matsumoto, K.; Sadakane, K.; Kidger, M.; et al. Authenticating the Presence of a Relativistic Massive Black Hole Binary in OJ 287 Using Its General Relativity Centenary Flare: Improved Orbital Parameters. *Astrophys. J.* **2018**, *866*, 11. [[CrossRef](#)]
10. Valtonen, M.J.; Sillanpää, A.; Haarala, S.; Valtaoja, L.; Valtaoja, E.; Sundelius, B.; Byrd, G.G.; Teräsanta, H.; Urpo, S. OJ 287 as a Binary System. In *Active Galactic Nuclei, Proceedings of the Conference Held at the Georgia State University, Atlanta, GA, USA, 28–30 October 1987*; Miller, H.R., Wiita, P.J., Eds.; Lecture Notes in Physics; Springer-Verlag: Berlin, Germany; New York, NY, USA, 1988; Volume 307, p. 68.
11. Sillanpää, A.; Haarala, S.; Valtonen, M.J.; Sundelius, B.; Byrd, G.G. OJ 287—Binary pair of supermassive black holes. *Astrophys. J.* **1988**, *325*, 628. [[CrossRef](#)]
12. Valtonen, M.J.; Lehto, H.J.; Sillanpää, A.; Nilsson, K.; Mikkola, S.; Hudec, R.; Basta, M.; Teräsanta, H.; Haque, S.; Rampadarath, H. Predicting the Next Outbursts of OJ 287 in 2006–2010. *Astrophys. J.* **2006**, *646*, 36. [[CrossRef](#)]
13. Sundelius, B.; Wahde, M.; Lehto, H.J.; Valtonen, M.J. A Numerical Simulation of the Brightness Variations of OJ 287. *Astrophys. J.* **1997**, *484*, 180. [[CrossRef](#)]
14. Ivanov, P.B.; Igumenshchev, I.V.; Novikov, I.D. Hydrodynamics of Black Hole-Accretion Disk Collision. *Astrophys. J.* **1998**, *507*, 131. [[CrossRef](#)]
15. Pihajoki, P. Black hole accretion disc impacts. *Mon. Not. R. Astron. Soc.* **2016**, *457*, 1145. [[CrossRef](#)]
16. Valtonen, M.J.; Ciprini, S.; Lehto, H.J. On the masses of OJ287 black holes. *Mon. Not. R. Astron. Soc.* **2012**, *427*, 77. [[CrossRef](#)]
17. Katz, J.I. A Precessing Disk in OJ 287? *Astrophys. J.* **1997**, *478*, 527. [[CrossRef](#)]
18. Tanaka, T.L. Recurring flares from supermassive black hole binaries: Implications for tidal disruption candidates and OJ 287. *Mon. Not. R. Astron. Soc.* **2013**, *434*, 2275. [[CrossRef](#)]
19. Britzen, S.; Fendt, C.; Witzel, G.; Qian, S.-J.; Pashchenko, I.N.; Kurtanidze, O.; Zajacek, M.; Martinez, G.; Karas, V.; Aller, M.; et al. OJ287: Deciphering the ‘Rosetta stone of blazars. *Mon. Not. R. Astron. Soc.* **2018**, *478*, 3199. [[CrossRef](#)]
20. Valtonen, M.J.; Lehto, H.J.; Nilsson, K.; Heidt, J.; Takalo, L.O.; Sillanpää, A.; Villforth, C.; Kidger, M.; Poyner, G.; Pursimo, T.; et al. A massive binary black-hole system in OJ287 and a test of general relativity. *Nature* **2008**, *452*, 851. [[CrossRef](#)] [[PubMed](#)]
21. Valtonen, M.; Zola, S.; Jermak, H.; Ciprini, S.; Hudec, R.; Dey, L.; Gopakumar, A.; Reichart, D.L.; Caton, D.B.; Gazeas, K.; et al. Polarization and Spectral Energy Distribution in OJ 287 during the 2016/17 Outbursts. *Galaxies* **2017**, *5*, 83. [[CrossRef](#)]
22. Valtonen, M.J.; Zola, S.; Ciprini, S.; Gopakumar, A.; Matsumoto, K.; Sadakane, K.; Kidger, M.; Gazeas, K.; Nilsson, K.; Berdyugin, A.; et al. Primary Black Hole Spin in OJ 287 as Determined by the General Relativity Centenary Flare. *Astrophys. J.* **2016**, *819*, L37. [[CrossRef](#)]
23. Valtonen, M.J. New Orbit Solutions for the Precessing Binary Black Hole Model of OJ 287. *Astrophys. J.* **2007**, *659*, 1074. [[CrossRef](#)]

24. Pihajoki, P.; Valtonen, M.; Zola, S.; Liakos, A.; Drozd, M.; Winiarski, M.; Ogloza, W.; Koziel-Wierzbowska, D.; Provencal, J.; Nilsson, K. Precursor Flares in OJ 287. *Astrophys. J.* **2013**, *764*, 5. [\[CrossRef\]](#)
25. Hudec, R.; Bašta, M.; Pihajoki, P.; Valtonen, M. The historical 1900 and 1913 outbursts of the binary blazar candidate OJ287. *Astron. Astrophys.* **2013**, *559*, A20. [\[CrossRef\]](#)
26. Wex, N. Testing Relativistic Gravity with Radio Pulsars. *arXiv* **2014**, arXiv:1402.5594.
27. Abbott, B.P.; Abbott, R.; Abbott, T.D.; Abernathy, M.R.; Acernese, F.; Ackley, K.; Adams, C.; Adams, T.; Addesso, P.; Adhikari, R.X.; et al. Tests of General Relativity with GW150914. *Phys. Rev. Lett.* **2016**, *116*, 221101. [\[CrossRef\]](#) [\[PubMed\]](#)
28. Abbott, B.P.; Abbott, R.; Abbott, T.D.; Acernese, F.; Ackley, K.; Adams, C.; Adams, T.; Addesso, P.; Adhikari, R.X.; Adya, V.B.; et al. Tests of General Relativity with GW170817. *arXiv* **2018**, arXiv:1811.00364.
29. Hees, A.; Do, T.; Ghez, A.M.; Martinez, G.D.; Naoz, S.; Becklin, E.E.; Boehle, A.; Chappell, S.; Chu, D.; Dehghanfar, A.; et al. Testing General Relativity with Stellar Orbits around the Supermassive Black Hole in Our Galactic Center. *Phys. Rev. Lett.* **2017**, *118*, 211101. [\[CrossRef\]](#) [\[PubMed\]](#)
30. Kormendy, J.; Bender, R. Supermassive black holes do not correlate with dark matter haloes of galaxies. *Nature* **2011**, *469*, 377. [\[CrossRef\]](#)
31. Valtonen, M.J.; Wiik, K. Optical polarization angle and VLBI jet direction in the binary black hole model of OJ287. *Mon. Not. R. Astron. Soc.* **2012**, *421*, 1861. [\[CrossRef\]](#)
32. Valtonen, M.; Pihajoki, P. A helical jet model for OJ287. *Astron. Astrophys.* **2013**, *557*, A28. [\[CrossRef\]](#)
33. Dey, L.; Valtonen, M.; Gopakumar, A.; Pihajoki, P. Modeling temporal variations of the jet position angle from jet precession in blazar OJ 287. In preparation.
34. Pietilä, H. Possibilities and Predictions of the OJ 287 Binary Black Hole Model. *Astrophys. J.* **1998**, *508*, 669. [\[CrossRef\]](#)
35. Valtonen, M.; Zola, S.; Pihajoki, P.; Enestam, S.; Lehto, H.J.; Dey, L.; Gopakumar, A.; Drozd, M.; Ogloza, W.; Zejmo, M.; et al. Accretion Disc Parameters determined from the General Relativity Centenary Flare of OJ287. In preparation.
36. Sakimoto, P.J.; Coroniti, F.V. Accretion disk models for QSOs and active galactic nuclei—The role of magnetic viscosity. *Astrophys. J.* **1981**, *247*, 19. [\[CrossRef\]](#)
37. Kramer, M.; Stairs, I.H.; Manchester, R.N.; McLaughlin, M.A.; Lyne, A.G.; Ferdman, R.D.; Burgay, M.; Lorimer, D.R.; Possenti, A.; D’Amico, N.; Sarkissian, J.M.; et al. Tests of General Relativity from Timing the Double Pulsar. *Science* **2006**, *314*, 97. [\[CrossRef\]](#)
38. Blanchet, L. Gravitational Radiation from Post-Newtonian Sources and Inspiralling Compact Binaries. *Living Rev. Relativ.* **2014**, *17*, 2. [\[CrossRef\]](#)
39. Will, C.M.; Maitra, M. Relativistic orbits around spinning supermassive black holes: Secular evolution to 4.5 post-Newtonian order. *Phys. Rev. D* **2017**, *95*, 064003. [\[CrossRef\]](#)
40. Blanchet, L.; Schafer, G. Gravitational wave tails and binary star systems. *Class. Quantum Gravity* **1993**, *10*, 2699. [\[CrossRef\]](#)
41. Yunes, N.; Siemens, X. Gravitational-Wave Tests of General Relativity with Ground-Based Detectors and Pulsar-Timing Arrays. *Living Rev. Relativ.* **2013**, *16*, 9. [\[CrossRef\]](#)
42. Berti, E.; Barausse, E.; Cardoso, V.; Gualtieri, L.; Pani, P.; Sperhake, U.; Stein, L.C.; Wex, N.; Yagi, K.; Baker, T.; et al. Testing general relativity with present and future astrophysical observations. *Class. Quantum Gravity* **2015**, *32*, 243001. [\[CrossRef\]](#)
43. Damour, T. 1974: The discovery of the first binary pulsar. *Class. Quantum Gravity* **2015**, *32*, 124009. [\[CrossRef\]](#)
44. Gürlebeck, N. No-Hair Theorem for Black Holes in Astrophysical Environments. *Phys. Rev. Lett.* **2015**, *114*, 151102. [\[CrossRef\]](#) [\[PubMed\]](#)
45. Thorne, K.S. Multipole expansions of gravitational radiation. *Rev. Mod. Phys.* **1980**, *52*, 299. [\[CrossRef\]](#)
46. Krishnendu, N.V.; Arun, K.G.; Mishra, C.K. Testing the Binary Black Hole Nature of a Compact Binary Coalescence. *Phys. Rev. Lett.* **2017**, *119*, 091101. [\[CrossRef\]](#) [\[PubMed\]](#)
47. Bambi, C.; Barausse, E. Constraining the Quadrupole Moment of Stellar-mass Black Hole Candidates with the Continuum Fitting Method. *Astrophys. J.* **2011**, *731*, 121. [\[CrossRef\]](#)
48. Johannsen, T.; Psaltis, D. Testing the No-hair Theorem with Observations in the Electromagnetic Spectrum. II. Black Hole Images. *Astrophys. J.* **2010**, *718*, 446. [\[CrossRef\]](#)
49. Valtonen, M.J.; Mikkola, S.; Lehto, H.J.; Gopakumar, A.; Hudec, R.; Polednikova, J. Testing the Black Hole No-hair Theorem with OJ287. *Astrophys. J.* **2011**, *742*, 22. [\[CrossRef\]](#)

50. Damour, T.; Gopakumar, A.; Iyer, B.R. Phasing of gravitational waves from inspiralling eccentric binaries. *Phys. Rev. D* **2004**, *70*, 064028. [[CrossRef](#)]
51. Königsdörffer, C.; Gopakumar, A. Phasing of gravitational waves from inspiralling eccentric binaries at the third-and-a-half post-Newtonian order. *Phys. Rev. D* **2006**, *73*, 124012. [[CrossRef](#)]
52. Tanay, S.; Haney, M.; Gopakumar, A. Frequency and time-domain inspiral templates for comparable mass compact binaries in eccentric orbits. *Phys. Rev. D* **2016**, *93*, 064031. [[CrossRef](#)]
53. Mikkola, S. A cubic approximation for Kepler's equation. *Celest. Mech.* **1987**, *40*, 329. [[CrossRef](#)]
54. Memmesheimer, R.-M.; Gopakumar, A.; Schäfer, G. Third post-Newtonian accurate generalized quasi-Keplerian parametrization for compact binaries in eccentric orbits. *Phys. Rev. D* **2004**, *70*, 104011. [[CrossRef](#)]
55. Klein, A.; Boetzel, Y.; Gopakumar, A.; Jetzer, P.; de Vittori, L. Fourier domain gravitational waveforms for precessing eccentric binaries. *Phys. Rev. D* **2018**, *98*, 104043. [[CrossRef](#)]
56. Arun, K.G.; Blanchet, L.; Iyer, B.R.; Sinha, S. Third post-Newtonian angular momentum flux and the secular evolution of orbital elements for inspiralling compact binaries in quasi-elliptical orbits. *Phys. Rev. D* **2009**, *80*, 124018. [[CrossRef](#)]
57. Valtaoja, E.; Teräsranta, H.; Tornikoski, M.; Sillanpää, A.; Aller, M.F.; Aller, H.D.; Hughes, P.A. Radio Monitoring of OJ 287 and Binary Black Hole Models for Periodic Outbursts. *Astrophys. J.* **2011**, *531*, 744. [[CrossRef](#)]
58. Valtonen, M.J.; Lehto, H.J.; Takalo, L.O.; Sillanpää, A. Testing the 1995 Binary Black Hole Model of OJ287. *Astrophys. J.* **2011**, *729*, 33. [[CrossRef](#)]
59. Valtonen, M.J.; Dey, L.; Hudec, R.; Zola, S.; Gopakumar, A.; Mikkola, S.; Ciprini, S.; Matsumoto, K.; Sadakane, K.; Kidger, M.; et al. High accuracy measurement of gravitational wave back-reaction in the OJ287 black hole binary. In Proceedings of the Gravitational Wave Astrophysics: Early Results from Gravitational Wave Searches and Electromagnetic Counterparts, Baton Rouge, LA, USA, 16–19 October 2017; Volume 338, pp. 29–36.
60. Villforth, C.; Nilsson, K.; Heidt, J.; Takalo, L.O.; Pursimo, T.; Berdyugin, A.; Lindfors, E.; Pasanen, M.; Winiarski, M.; Drozd, M.; et al. Variability and stability in blazar jets on time-scales of years: Optical polarization monitoring of OJ 287 in 2005–2009. *Mon. Not. R. Astron. Soc.* **2018**, *402*, 2087. [[CrossRef](#)]
61. Qian, S. Model simulation of optical light curves for blazar OJ287. *arXiv* **2019**, arXiv:1904.03357.
62. Goyal, A.; Stawarz, Ł.; Zola, S.; Marchenko, V.; Soida, M.; Nilsson, K.; Ciprini, S.; Baran, A.; Ostrowski, M.; Wiita, P.J.; et al. Stochastic Modeling of Multiwavelength Variability of the Classical BL Lac Object OJ 287 on Timescales Ranging from Decades to Hours. *Astrophys. J.* **2018**, *863*, 175. [[CrossRef](#)]
63. Valtonen, M.J. The OJ 287 Binary Model and the Expected Outburst in November 1995. Available online: <http://adsabs.harvard.edu/abs/1996wtvi.conf...64V> (accessed on 6 May 2019).

